

# SEISMIC QUALITY FACTOR ESTIMATION USING CONTINUOUS WAVELET TRANSFORM

*Yanhui Zhou<sup>1</sup>, Wei Zhao<sup>2</sup>, Yan Ge<sup>1</sup>, Jinghuai Gao<sup>1</sup>, Xiaokai Wang<sup>1</sup>, Chenyang Ge<sup>1</sup>*

<sup>1</sup> Institute of Wave and Information, Xi'an Jiaotong University, Xi'an, China, 710049

<sup>2</sup>CNOOC, Beijing, China, 100027

## 1. INTRODUCTION

When propagating in the Earth, seismic wave will be attenuated. Usually the seismic attenuation can be quantified by quality factor  $Q$ . The direct estimations of  $Q$  in Fourier frequency domain include logarithm spectral ratio [1], centroid frequency shift (CFS) [2], and peak frequency shift methods [3]. In these methods, before calculating its spectrum in Fourier domain, the recording will be truncated by a time window. If the time window is inappropriate, the estimated  $Q$  may deviate more from accurate value. Based on Gabor-Morlet transform, the  $Q$  estimation [4] can avoid the problem of time window. By continuous wavelet transform (CWT), the relationship between peak scale of the scalogram in wavelet domain and  $Q$  is derived [5], and it can be used to estimate  $Q$  accurately. However, the relationship is based on the assumption of impulse source wavelet.

In this paper, we assume source being a constant-phase and develop a formula of frequency-independent  $Q$  estimation by the ratio of wavelet-domain peak amplitude. And Morlet wavelet is selected as mother wavelet in CWT. Finally, we test our formula by synthetic and real zero-offset VSP data.

## 2. METHODOLOGY

If source wavelet is constant-phase, its corresponding frequency-domain expression can be written as

$$U(\omega; 0) = \exp[-(\omega - \sigma_0)^2 / (2\delta_0^2) + i\varphi_0], \quad (1)$$

where,  $\sigma_0$  and  $\delta_0$  denote the dominant (angular) frequency and standard deviation, respectively, and phase  $\varphi_0$  is a constant. In real VSP data test,  $\sigma_0$ ,  $\delta_0$  and  $\varphi_0$  in (1) are usually unknown and should be estimated previously.

When the source wavelet propagating in the anelastic media with frequency-independent  $Q$ , the frequency-domain signal can be expressed as

$$U(\omega; t) = U(\omega; 0) \exp[-i\omega t - \omega t / (2Q)], \quad (2)$$

where,  $i = \sqrt{-1}$ ,  $\omega$  is angular frequency,  $t$  is travel time. Performing CWT in frequency domain on  $U(\omega; t)$  gives [6]

$$W[\psi; U](b, a) = [1/(2\pi)] \cdot \int_{-\infty}^{\infty} U(\omega; t) [\sqrt{a} \hat{\psi}(a\omega) \exp(-i\omega b)]^* d\omega, \quad (3)$$

where,  $b, a$  are translation and scale factor respectively,  $\sqrt{a} \hat{\psi}(a\omega) \exp(-i\omega b)$  denotes the Fourier transform of wavelet function family  $\psi((t-b)/a)/\sqrt{a}$ , and the asterisk means the conjugate. If Morlet wavelet is selected,  $\hat{\psi}(a\omega)$  is rewritten as

$$\hat{\psi}(a\omega) = \exp[-(a\omega - \sigma)^2], \quad (4)$$

where,  $\sigma$  is modulated frequency. And in this paper, we select  $\sigma$  as 6.0. Substituting of (1) and (4) into (3) and with the fixed scale  $a$ , then let  $b=t$ , we will obtain the wavelet-domain peak amplitude  $|W[\psi;U](a)|_{\max}$  of  $W[\psi;U](b,a)$  [5]

$$|W[\psi;U](a)|_{\max} = \sqrt{a} \cdot \exp\{-[\sigma_0^2/(2\delta_0^2) + \sigma^2]\} \cdot \exp\left\{\frac{[\sigma_0/(2\delta_0^2) - t/(4Q) + a\sigma]^2}{[1/(2\delta_0^2) + a^2]}\right\} / \sqrt{4\pi[1/(2\delta_0^2) + a^2]}. \quad (5)$$

Suppose the reference and target recorded wavelets are  $U_1(\omega;t_1)$  and  $U_2(\omega;t_2)$ , respectively, and the corresponding travel times are  $t_1$  and  $t_2$  ( $t_2 > t_1$ ); in terms of (5), the ratio of wavelet-domain peak amplitude of these two recordings generates

$$\frac{|W[\psi;U_2](a)|_{\max}}{|W[\psi;U_1](a)|_{\max}} = \exp\left\{\frac{-\Delta t \cdot [(\sigma_0/\delta_0^2 + 2a\sigma) - (t_1/(2Q) + \Delta t/(4Q))]}{4Q \cdot [1/(2\delta_0^2) + a^2]}\right\}, \quad (6)$$

where, travel time interval  $\Delta t = t_2 - t_1$ . Usually  $Q$  value is more than 10.0 and the value of  $t_1$ ,  $\Delta t$  are considerably small, so the exponential term  $t_1/(2Q) + \Delta t/(4Q)$  in the right side of (6) will meet  $t_1/(2Q) + \Delta t/(4Q) \ll \sigma_0/\delta_0^2 + 2a\sigma$  and can be omitted here. And then we changes (6) into

$$\frac{|W[\psi;U_2](a)|_{\max}}{|W[\psi;U_1](a)|_{\max}} = \exp\left\{\frac{-\Delta t \cdot (\sigma_0/\delta_0^2 + 2a\sigma)}{4Q \cdot [1/(2\delta_0^2) + a^2]}\right\}, \quad (7)$$

taking natural logs of the two sides of (7) gives

$$\ln(|W[\psi;U_2](a)|_{\max} / |W[\psi;U_1](a)|_{\max}) = \frac{-\Delta t \cdot [\sigma_0/(2\delta_0^2) + a\sigma]}{2Q \cdot [1/(2\delta_0^2) + a^2]}; \quad (8)$$

then make the variable  $\eta = [\sigma_0/(2\delta_0^2) + a\sigma]/[1/(2\delta_0^2) + a^2]$ , (8) will be rewritten as

$$-\ln(|W[\psi;U_2](a)|_{\max} / |W[\psi;U_1](a)|_{\max}) = \Delta t \cdot \eta / 2Q. \quad (9)$$

If the standard deviation  $\delta_0$  approaches the infinity, (9) will be changed to

$$-\ln(|W[\psi;U_2](a)|_{\max} / |W[\psi;U_1](a)|_{\max}) = \Delta t \cdot \sigma / (2aQ), \quad (10)$$

and (10) is the  $Q$  estimation formula when the source wavelet is an impulse.

In this paper, we discretize the scale factor  $a$  as a set of scales  $a = a_0 2^{-(j-1) \times 0.125}$ ,  $j = 1, \dots, J$ , where  $a_0$  and  $J$  are the largest scale and the number of discrete scales, respectively. And  $a_0$  and  $J$  are determined by the usable bandwidth of source wavelet. In terms of (9), by plotting  $-\ln(|W[\psi;U_2](a)|_{\max} / |W[\psi;U_1](a)|_{\max})$  as a function of variable  $\Delta t \cdot \eta / 2$  and fitting a straight line using least-square linear regression,  $Q$  can be obtained from the slope of the fitted line.

### 3. EXAMPLES

#### 3.1. Synthetic Zero-offset VSP Data

We calculate the synthetic zero-offset VSP data with the dominant frequency and standard deviation of constant-phase source wavelet set as  $\sigma_0 = 60\pi$  and  $\delta_0 = 75$ , respectively, and for simplicity, phase as  $\varphi_0 = 0$ . We chose the effective frequency range of recordings as 15-80Hz; then the maximum and minimum of scale factor  $a$  are evaluated as 0.064 and 0.012, and  $J = 19$ . In Fig. 1(a), the depth interval between two adjacent geophones is 20 m and the depth range is 400 m to 1600 m. In Fig. 1(b) only the direct wave is considered and the sampling rate is 1 KHz. We display the  $Q$  estimation of the first and second layer by least-square linear regression, in terms of (9) and (10), respectively, in Fig. 2 and 3. In the first layer the  $Q$  values are obtained as 105.0 and 139.5. In the second layer, the estimated  $Q$  value is 52.0 and 69.3, respectively. Comparing with the exact  $Q$  values given in Fig. 1(a), we can find that when the source is modeled by a constant-phase wavelet in (1), the estimated  $Q$  value by (9) will be more accurate than that by (10) of impulse source wavelet.

### 3.2. Real Zero-offset VSP Data

The real zero-offset VSP data are gathered in the Sulige gas field of the northwest district of China. The geophones are located with 5 m interval. Fig. 4(a) shows the recordings with sampling frequency being 1KHz. By the classic Newton iteration method,  $\sigma_0$  and  $\delta_0$  are estimated as  $\sigma_0 = 60\pi$ ,  $\delta_0 = 70$ . As  $\sigma_0$ ,  $\delta_0$  approach to that of source wavelet in synthetic example, we chose the same  $a$  as that used in the synthetic. In terms of velocity and geological profile, the depth interval can be subdivided into five layers approximately. Within each layer, we estimate  $Q$  from different recording pairs comparison by (9), (10) and CFS method [4] respectively, and then we regard the median of obtained reasonable  $Q$  values, i.e. positive value, as the corresponding layer-  $Q$ . The final layer-  $Q$  is shown in Fig. 4(b) and the gray circles indicate the distribution of gas reservoirs. We can notice that  $Q$  value estimated by (9) (the solid line) is very similar to that estimated by CFS (the solid line marked by crossings), however,  $Q$  values estimated by (10) (the solid line marked by boxes) deviate more. In the fourth layer of gas accumulation,  $Q$  value estimated by (9) is approximately 30, which is lower and very near to the estimated  $Q$  values in [7].

## 4. DISCUSSION AND CONCLUSION

With the assumption of constant-phase source wavelet, based on the one-way wave propagation theory in anelastic media and CWT, the formula of frequency-independent  $Q$  estimation in wavelet domain is derived. The examples of synthetic zero-offset VSP data demonstrate that when the source is constant-phase wavelet, the estimated  $Q$  value by using our formula is nearer to the true value than that by the formula of impulse source. The results of real zero-offset VSP indicate that our method provides more accurate  $Q$  information than that based on impulse source. And also the corresponding layer-  $Q$  is consistent with well log, which may aid in the interpretation of gas reservoirs characteristics and lithological discrimination. Although the variation of  $Q$  value estimated by (10) is similar to that of  $Q$  estimated by our formula,  $Q$  value estimated by (10) is unreliable, which may cause appreciable deviation in inverse- $Q$  filtering.

## 5. ACKNOWLEDGEMENT

We thank NNSF of China (40730424, 40674064), China National 863 Program (2006AA09A102-11) and National Science & Technology Major Project (2008ZX05023-005-005, 2008ZX05025-001-009)

## 6. REFERENCES

- [1] M. P. Matheney and R. L. Nowack, "Seismic attenuation values obtained from instantaneous frequency matching and spectral ratios," *Geophys. J. Int.*, vol. 123, no. 1, pp. 1-15, Oct. 1995.
- [2] Y. Quan and J. M. Harris, "Seismic attenuation tomography using the frequency shift method," *Geophysics*, vol. 62, no. 3, pp. 895-905, Jul. 1997.
- [3] C. J. Zhang and T. J. Ulrych, "Estimation of quality factors from CMP records," *Geophysics*, vol. 67, no. 5, pp. 1542-1547, Sep. 2002.
- [4] M. T. Taner, "Joint time/frequency analysis,  $Q$  quality factor and dispersion computation using Gabor-Morlet wavelet or Gabor-Morlet transform," *Rock Solid Images*, pp. 1-5, 1983.
- [5] H. B. Li, W. Z. Zhao, H. Cao, F. C. Yao, and L. Y. Shao, "Measures of scale based on the wavelet scalogram with applications to seismic attenuation," *Geophysics*, vol. 71, no. 5, pp. V111-V118, Sep. 2006.
- [6] S. A. Mallat, *Wavelet Tour of Signal Processing*. New York: Academic Press Inc, 1999.
- [7] S. L. Yang and J. H. Gao, "Seismic quality factors estimation from spectral correlation," *IEEE Trans. Geoscience and Remote sensing Letters*, vol. 5, no. 4, pp.740-744, Oct. 2008.
- [8] Y. H. Wang, "Quantifying the effectiveness of stabilized inverse  $Q$  filtering," *Geophysics*, vol. 68, no. 1, pp. 337-345, Jan. 2003.

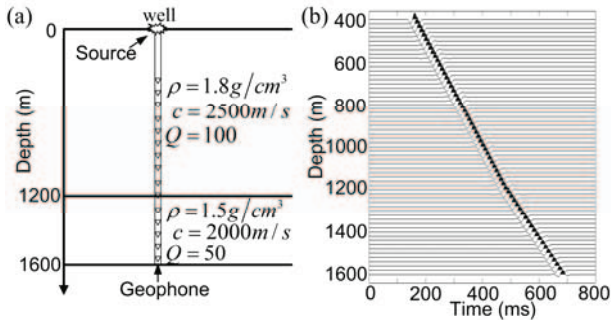


Fig.1 The synthetic zero-offset VSP data: (a) two-layer depth model; (b) the synthetic VSP section.

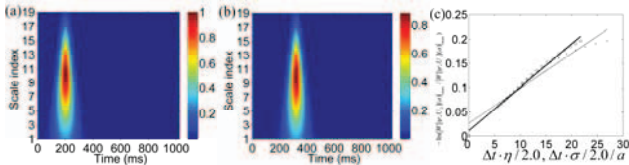


Fig. 2  $Q$  estimation in the first layer of the synthetic VSP: (a) and (b) are the wavelet-domain amplitude spectrum  $|W[\psi; U_1](a)|, |W[\psi; U_2](a)|$  of VSP recording at depth of 500 m and 800 m respectively; (c) the natural logs of wavelet-domain peak amplitude ratio. In Fig. 2(c) and in the following Fig. 3(c), thicker and thinner black lines are the fitted lines corresponding to (9) and (10), respectively.

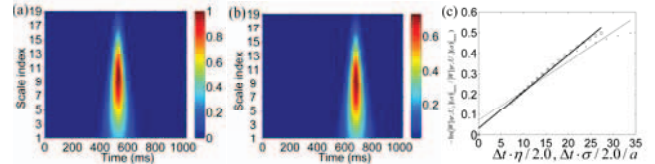


Fig. 3  $Q$  estimation in the second layer of the synthetic VSP: (a) and (b) are the wavelet-domain amplitude spectrum of VSP recording at depth of 1300 m and 1600 m, respectively; (c) the natural logs of wavelet-domain peak amplitude ratio.

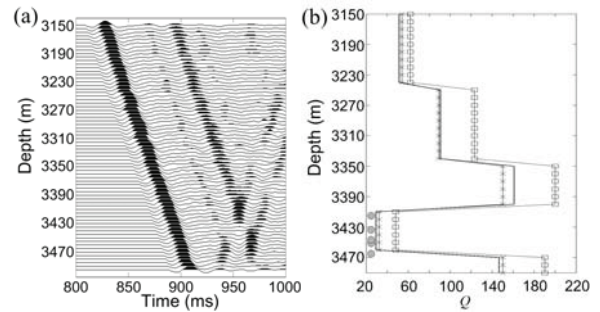


Fig. 4 the  $Q$  estimation of real zero-offset VSP data: (a) the real zero-offset VSP recordings; (b) the estimated layer- $Q$  value by (9)(solid line), (10)(solid line marked by boxes), and CFS (solid line marked by crossings) respectively, and the grey circles denote the gas reservoirs.